

Quantifying Aromaticity at the Molecular and Supramolecular Limits: Comparing Homonuclear, Heteronuclear, and H-Bonded Systems

Abdul Rehaman, Ayan Datta, Sairam S. Mallajosyula, and Swapan K. Pati*

*Theoretical Sciences Unit and Chemistry and Physics of Materials Unit,
Jawaharlal Nehru Centre for Advanced Scientific Research, Jakkur Campus,
Bangalore 560 064, India*

Received June 22, 2005

Abstract: The aromatic/antiaromatic characteristics of B–N and P–N analogues of benzene and cyclobutadiene have been studied using quantum chemical methods. We use established parameters such as nucleus-independent chemical shifts, charge density at the ring critical point, and stabilization energies to quantify the nature of interactions in these molecular systems. $B_3N_3H_6$ and $N_3P_3F_6$ resemble benzene in being aromatic, albeit to a lesser extent, while $B_2N_2H_4$ and $N_2P_2F_4$ are found to be aromatic, opposite to that for cyclobutadiene. A σ – π separation analysis has been performed to critically examine the contributions from the π electrons compared to that from the σ backbone. The structural aspects in the weak interaction limits such as the H-bonded cyclic trimers of HX ($X = F, Cl, \text{ and } Br$) have also been investigated. Even in such weak interaction limits, these cyclic systems are found to be substantially stable. These H-bonded systems exhibit nonlocal polarizations across the full-perimeter of the ring that lead to aromaticity. We propose the term “*H-bonded aromaticity*” for such closed-loop weakly delocalized systems. This new formalism of aromaticity has the potential to explain structures and properties in supramolecular systems.

I. Introduction

Aromaticity is a well-known and useful concept in organic chemistry. Though the initial interpretation of aromaticity was based only on one-electron theories such as the Hückel model, modern quantum chemical calculations have now established this concept on a firm footing.¹ The rapid synthesis and characterization of new molecules exhibiting aromaticity/antiaromaticity have further fueled the interest in these systems.^{2,3} From the conventional rules of aromaticity/antiaromaticity in organic molecules, the concept has been recently introduced to all-metal clusters with the proposal of d-orbital aromaticity and σ aromaticity.^{4–6} The past decade has also witnessed a renewed interest in concepts such as Möbius aromaticity with the synthesis of molecular Möbius systems.⁷ Also in the same context, three-dimensional aromaticity in molecular complexes has led to the

stabilization of many otherwise unstable molecular systems⁸ and organometallic sandwich complexes, for example, dinuclear Zn complexes ($Cp^*_2-Zn_2$) ($Cp = \text{cyclopentadiene}$).⁹

Central to the concept of aromaticity and antiaromaticity is the simple yet widely successful Hückel rule that predicts $(4n + 2)\pi$ planar electronic systems to be aromatic and stable, while $4n\pi$ electronic systems are antiaromatic and unstable. The Hückel rule is very successful in representative organic molecules such as benzene and cyclobutadiene. It is also quite applicable to heterocyclic organic molecules.¹⁰ However, the application of the rule cannot be extended to the realms of inorganic molecules. The aromaticity in inorganic molecules such as borazine and phosphazene has been a long-debated issue. For example, though $B_3N_3H_6$ and $N_3P_3F_6$ have a resemblance to benzene, both in structure and reactivity, these molecules differ substantially from benzene, and such differences have been widely reported in the literature.¹¹ However, for the four-membered ring systems

* Corresponding author e-mail: pati@jncasr.ac.in.

such as $B_2N_2H_4$ and $N_2P_2F_4$, synthesis has been quite difficult, and only a few four-membered ring systems with sterically hindered ligands have been realized so far.¹² Thus, in the $4n\pi$ manifold of these charge transfer (CT) complexes, the structure–property relationship is yet to be fully understood.

For the present work, we consider various four- and six-membered rings of homonuclear and heteronuclear systems. These rings are either stabilized through a complete delocalization of the π electrons (as for homonuclear systems) or through a partial or complete charge transfer of π electrons due to electronegativity differences between the atoms (as for heteronuclear systems). We also consider a class of cyclic systems where the stabilization is due to weak hydrogen-bonding interactions. H-bonded interactions are known to follow directionality,^{13,14} and on the basis of graph theory analyses,^{15,16} it has been suggested that cyclic polygonal closed-loop structures are stable geometries for H-bonded molecules. Similar conclusions are also derived from modern quantum chemical calculations.¹⁷ The nature of σ -electron delocalizations and, thus, aromaticity has been critically examined for such molecules. We, thus, compare and contrast the aromaticity or the lack of it in complexes ranging from purely covalent, to ionic, to partially ionic, to weakly interacting systems.

In the next section, we perform ab initio calculations on the homoatomic (C_6H_6 and C_4H_4) and heteroatomic ($B_3N_3H_6$, $N_3P_3F_6$, $B_2N_2H_4$, and $N_2P_2F_4$) systems. Following the calculations, we critically examine the aromaticity/antiaromaticity characteristics for these systems along with the weakly interacting H-bonded systems. We then critically examine the role of the delocalized π electrons and the σ framework in rationalizing the stability for the molecular structures. Finally, we conclude the paper with a summary of the results.

II. Computational Details and Results

All the geometries for the molecular systems considered in this work have been fully optimized at the density functional theory (DFT) level using the Becke, Lee, Yang, and Parr three-parameter correlation functional (B3LYP) at the 6-311G++(d,p) basis set level.¹⁸ All the calculations have been performed using the Gaussian 03 set of programs.¹⁹ Additional calculations at the MP2 level have been performed to further verify the structures for these molecules. Also, frequency calculations are performed to confirm the ground-state structures (see Supporting Information).

In Figure 1, the optimized structures for all the π -delocalized systems are shown. It is seen that, for the homoatomic systems, C_6H_6 and C_4H_4 (Figure 1a and b), the bond-length alterations (BLAs; defined as the average difference between the bond lengths of two consecutive bonds) are 0.00 and 0.24 Å, representing aromatic and antiaromatic features, respectively. The six-membered heteroatomic clusters, $B_3N_3H_6$ and $N_3P_3F_6$ (Figure 1c and e), have a 0 BLA high-symmetric hexagonal structure. For the four-membered rings, $B_2N_2H_4$ and $N_2P_2F_4$ (Figure 1d and f), the structures are rhombohedral with equal bond lengths and unequal diagonal lengths. For $B_2N_2H_4$, the shorter and longer diagonals are 1.90 and 2.15 Å, respectively, and for $N_2P_2F_4$, they are 2.15 and 2.47 Å, respectively. Thus, for the homoatomic C_4H_4 , John–Teller

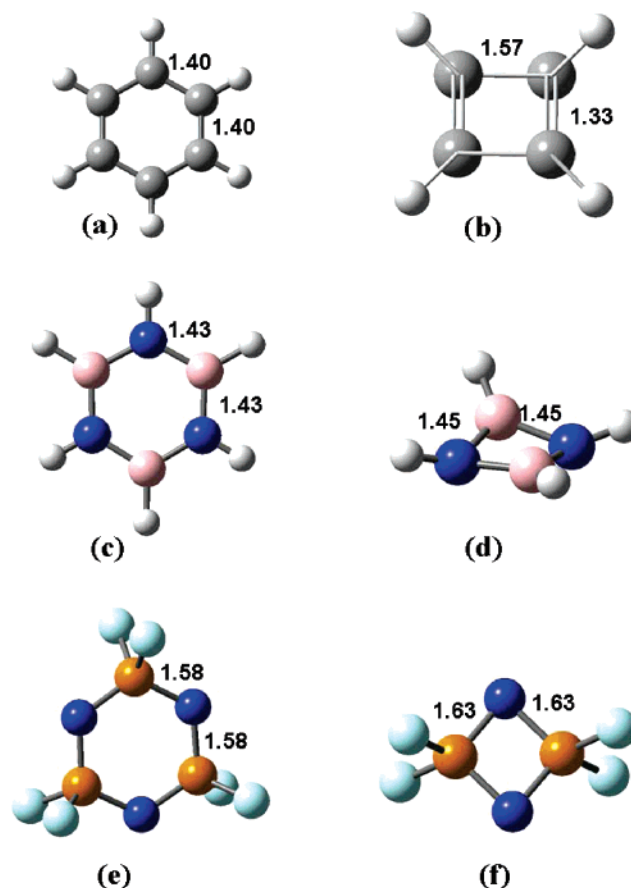


Figure 1. Ground-state optimized geometries of (a) C_6H_6 , (b) C_4H_4 , (c) $B_3N_3H_6$, (d) $B_2N_2H_4$, (e) $N_3P_3F_6$, and (f) $N_2P_2F_4$. Bond lengths in Å shown for each structure.

(JT) distortion leads to a rectangular geometry from a square geometry, while for the heteroatomic four-membered ring systems, such distortions lead to a rhombohedral geometry.

In Figure 2, we show the highest occupied molecular orbitals (HOMO) for the above-mentioned molecular systems. For the homoatomic molecular systems such as C_6H_6 and C_4H_4 (Figure 2a and b), the nodal plane passes through the bonds and the MO is delocalized over each atom. But, for $B_3N_3H_6$ and $N_3P_3F_6$ (Figure 2c and e), the MOs are indicative of electronegativity differences. For the four-membered ring systems, $B_2N_2H_4$ and $N_2P_2F_4$ (Figure 2d and f), very large contributions are observed for the N atoms and negligible contributions from the electropositive atoms are observed, suggesting CT from the N orbital to the vacant orbitals (p_z orbital of B and d_{xz} and d_{yz} orbitals of P). As expected on the basis of symmetry and relative electronegativities, for $B_2N_2H_4$ (Figure 2d), the node passes through the less electronegative B atoms. In sharp contrast, the node passes through the longer C–C bonds for C_4H_4 (Figure 2b).

The case of the four-membered B–N compound, $B_2N_2H_4$, requires a special mention. The ground-state structure corresponds to a puckering of 17.3° from planarity. However, the bond lengths are all equivalent, suggesting that the lone pair of electrons on the N atom are localized and are not transferred to the nearby B atom, and a resonance form similar to that for C_4H_4 (two alternate short and long bonds) is not realized. In fact, the planar structure for $B_2N_2H_4$ is

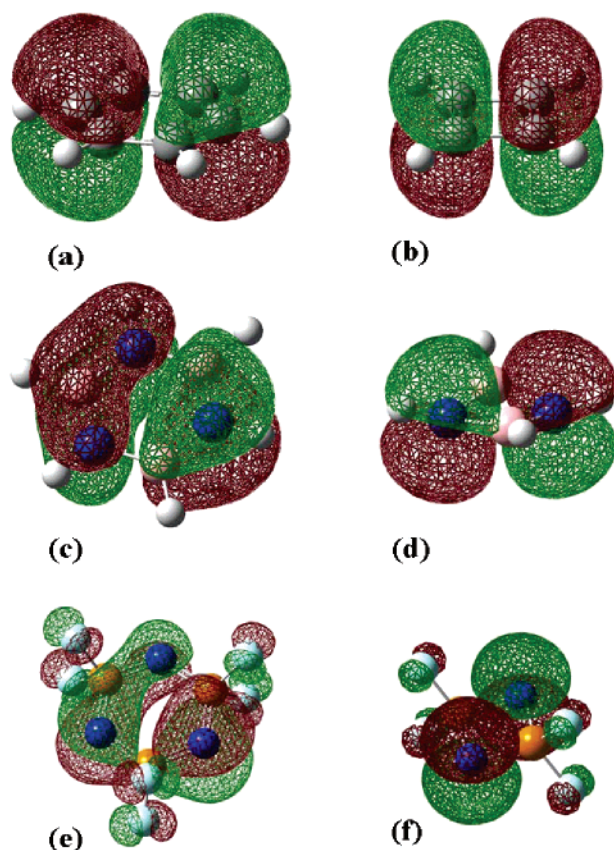


Figure 2. Highest occupied molecular orbitals (HOMOs) of (a) C_6H_6 , (b) C_4H_4 , (c) $B_3N_3H_6$, (d) $B_2N_2H_4$, (e) $N_3P_3F_6$, and (f) $N_2P_2F_4$.

1.00 kcal/mol higher in energy compared to the puckered structure and has one imaginary frequency corresponding to the out-of-plane bending mode of the atoms. However, a difference of 1 kcal/mol in energies between these two structures is comparable to the thermal energy at room temperature (0.6 kcal/mol). Thus, there is a possibility for such four-membered rings to exist in two different polymorphs: the planar and the puckered forms. We performed a search for such polymorphs in the Cambridge Crystallographic Database²⁰ (CCSD) for the four-membered B_2N_2 ring systems and had 47 hits. Of them, two compounds show polymorphism in the ring structure. For example, the crystal of 1,3-di-*tert*-butyl-2,4-bis(pentafluorophenyl)-1,3,2,4-diazadiboretidine (CCSD code: BFPDZB) crystallizing in an $I2/c$ point group has a planar B_2N_2 unit,²¹ while the tetrakis-(*tert*-butyl)-1,3,2,4-diazadiboretidine crystal (CCSD code: CETTAW) with a point group of Pc maintains a puckered B_2N_2 unit with a puckering angle of 18° .²² Note that our computed structure also has a similar puckering angle. Thus, the existence of the two crystal polymorphs in the B_2N_2 unit strongly support our calculations.

III. Aromaticity Criteria

For a quantitative measurement of aromaticity/antiaromaticity in these systems, we have calculated the nucleus-independent chemical shifts (NICS) at the center of each ring structure. Compounds with exalted diamagnetic susceptibility are aromatic, while those showing paramagnetic susceptibilities

Table 1. Magnitudes of Bond Length Alteration (BLA) in Å, Stabilization Energies in kcal/mol (ΔE), Nucleus-Independent Chemical Shift (NICS) in ppm, Charge Density at the Ring Critical Point (ρ_{RCP}) in $e/\text{\AA}^3$ Units, and Laplacian of the Charge Density ($\nabla^2\rho_{RCP}$) in $e/\text{\AA}^5$ Units for the Systems Considered in the Present Study

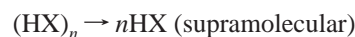
systems	BLA	ΔE	NICS	ρ_{RCP}	$\nabla^2\rho_{RCP}$
C_6H_6	0.00	-219.36	-8.072	0.022	0.161
C_4H_4	0.24	-52.29	35.763	0.102	0.458
$B_3N_3H_6$	0.00	-142.16	-1.595	0.020	0.119
$B_2N_2H_4$	0.00	-49.35	-2.921	0.099	0.369
$N_3P_3F_6$	0.00	-238.51	-6.912	0.020	0.095
$N_2P_2F_4$	0.00	-105.61	-10.874	0.104	0.210
$(HF)_3$	0.90	-10.94	-2.94	0.008	0.046
$(HCl)_3$	1.29	-4.23	-1.98	0.002	0.006
$(HBr)_3$	1.35	-1.67	-1.89	0.002	0.006

are antiaromatic.²³ Also, another parallel method to characterize aromaticity/antiaromaticity is to calculate the charge density (ρ_{RCP}) and its Laplacian ($\nabla^2\rho_{RCP}$) at the ring critical point. In general, molecules with similar architecture share similar topological features and, thus, serve as a tool for understanding structural aspects in molecules. There have been intense efforts to relate these topological aspects with aromaticity/antiaromaticity criteria recently.²⁴

In Table 1, we tabulate the magnitudes of the BLA, stabilization energies, NICS, ρ_{RCP} , and $\nabla^2\rho_{RCP}$ for all the systems. We calculate the stabilization energies as the difference in energy between the molecules reported and the independent fragments such as



These reported energies are corrected for thermal parameters



(zero-point energies and the entropy corrections). Note that the stabilization energies for the weakly interacting systems are corrected for basis set superposition errors using counterpoise corrections.²⁵

We first discuss the magnetic criteria for characterizing aromaticity/antiaromaticity in these systems. As evident from Table 1, all the systems except C_4H_4 show aromaticity (negative NICS). Among the six-membered rings, the aromaticity in the systems follows the order $C_6H_6 > N_3P_3F_6 > B_3N_3H_6$, following the order of decreasing covalency in these systems. For C_6H_6 , the conjugation is most effective because of $p\pi$ - $p\pi$ overlap, while it decreases for $N_3P_3F_6$, because of less-effective $p\pi$ - $d\pi$ overlap. For borazine, however, such orbital overlap is poor, and the stabilization in $B_3N_3H_6$ is primarily due to CT from N to B. In the four-membered systems, aromaticity follows the order $N_2P_2F_4 > B_2N_2H_4 > C_4H_4$ (antiaromatic). The decrease in aromaticity from $N_2P_2F_4$ to $B_2N_2H_4$ arises as a result of stronger covalency in the N-P bond compared to that of the B-N bond.

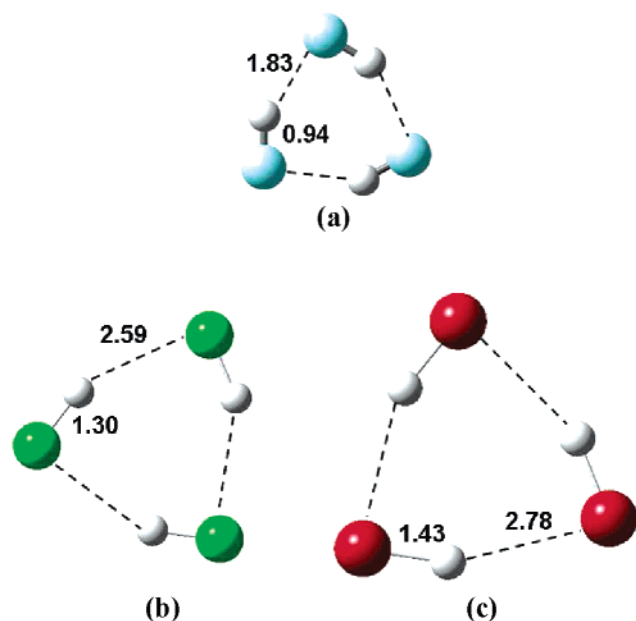


Figure 3. Ground-state optimized geometries of weakly interacting systems (a) $(\text{HF})_3$, (b) $(\text{HCl})_3$, and (c) $(\text{HBr})_3$. Bond lengths in Å are shown for each structure.

In Figure 3, we report the ground-state optimized geometries of the weakly interacting systems: $(\text{HX})_3$, ($\text{X} = \text{F}$, Cl , and Br). $(\text{HF})_3$ forms the most compact cyclic structure (as evident from the stabilization energies and BLA), followed by $(\text{HCl})_3$ and $(\text{HBr})_3$. All three of these H-bonded systems have a stable ground-state cyclic geometry, as evident from the absence of any imaginary frequencies in their optimized structures (see Supporting Information). Thus, there is a predominating tendency for these systems to assume a cyclic geometry. This is, in principle, identical to the origin of the high symmetric 0 BLA structures of the conventional aromatic systems such as benzene. The existence of aromaticity is evident from the NICS values (in ppm) of -2.94 , -1.98 , and -1.89 for $(\text{HF})_3$, $(\text{HCl})_3$, and $(\text{HBr})_3$, respectively. The decreasing aromaticity in the series follows the trend of their decreasing strength of H bonding and the stability of the cyclic H-bonded systems.

The issue of aromaticity in H-bonded systems has been dealt with in the literature in the context of resonance-assisted H bonding for π -conjugated systems such as the enol form of β -diketone.²⁶ For example, the *cis*-2-enol form of acetylacetone, where the proton is shared equally by the two O atoms, corresponds to the ground-state geometry.²⁷ The stability of these structures is understood on the basis of the formation of a six-membered ring containing 6π electrons and, thus, aromatic characteristics. However, note that, for our $(\text{HX})_3$ systems, the stability has its origins in the delocalization of the σ electrons. The stabilization energies (after incorporation of zero-point and entropy corrections) associated with such σ aromaticity in $(\text{HF})_3$, $(\text{HCl})_3$, and $(\text{HBr})_3$ are -10.94 , -4.23 , and -1.67 kcal/mol, respectively.

For a quantitative estimation of the role of H bonding in introducing polarization across the full perimeter of these cyclic systems, we calculate the polarizabilities for these systems as $\alpha_{\text{ring}} = \bar{\alpha}_{\text{trimer}} - 3\bar{\alpha}_{\text{monomer}}$, where we define the

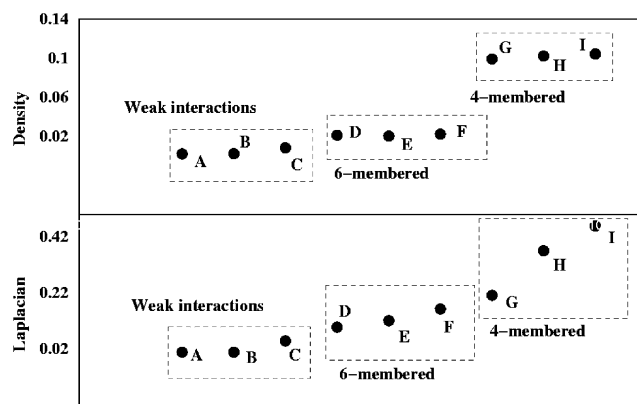


Figure 4. Charge density (upper panel) and laplacian of the charge density (lower panel) at the ring critical points of (A) $(\text{HCl})_3$, (B) $(\text{HBr})_3$, (C) $(\text{HF})_3$, (D) $\text{B}_3\text{N}_3\text{H}_6$, (E) $\text{N}_3\text{P}_3\text{F}_6$, (F) C_6H_6 , (G) $\text{B}_2\text{N}_2\text{H}_4$, (H) C_4H_4 , and (I) $\text{N}_2\text{P}_2\text{F}_4$.

isotropic average polarizability for the trimer and monomer as

$$\bar{\alpha} = \frac{1}{3} \sum_i (\alpha_{ii}) \quad (1)$$

where the sums are over the coordinates x , y , and z ($i = x$, y , and z). The calculated polarizabilities are $\bar{\alpha}_{\text{ring}}(\text{HF}) = +2.24$ au, $\bar{\alpha}_{\text{ring}}(\text{HCl}) = +7.97$ au, and $\bar{\alpha}_{\text{ring}}(\text{HBr}) = +12.16$ au. Note that, for all three of the H-bonded complexes, there is a cooperative enhancement of polarizability, suggesting extended delocalization across the ring. Also, the order of increasing polarizability, $\bar{\alpha}_{\text{ring}}(\text{HF}) < \bar{\alpha}_{\text{ring}}(\text{HCl}) < \bar{\alpha}_{\text{ring}}(\text{HBr})$, follows the decreasing electronegativity in X along group 17 of the periodic table. This leads to a more facile delocalization of σ electrons for the weaker H-bonded systems as compared to the strongest H bonding in HF . However, the aromaticity index (NICS) suggests larger aromaticity for HF and HCl compared to HBr primarily because of a more compact structure (smaller surface area), leading to stronger diamagnetic ring current.

An analysis of the charge density (ρ_{RCP}) and the Laplacian of the charge density ($\nabla^2\rho_{\text{RCP}}$) at the ring critical points for these systems reveals clear distinctions between the nature of interactions in the rings (Figure 4). Both ρ_{RCP} and $\nabla^2\rho_{\text{RCP}}$ show maximum localizations for the four-membered rings C_4H_4 , $\text{B}_2\text{N}_2\text{H}_4$, and $\text{N}_2\text{P}_2\text{F}_4$, followed by the six-membered rings C_6H_6 , $\text{B}_3\text{N}_3\text{H}_6$, and $\text{N}_3\text{P}_3\text{F}_6$ (see Table 1 for the values for each system). The H-bonded systems also show a localization of electrons at the ring critical points, suggesting substantial stability in these cyclic systems, supporting results derived from our NICS calculations. Consistent with the maximum stability of the $(\text{HF})_3$ H-bonded system, both ρ_{RCP} and $\nabla^2\rho_{\text{RCP}}$ are also highest for it. Thus, both NICS and topological aspects suggest substantial electronic delocalizations across the weakly interacting rings.

IV. σ - π Separation Analysis

As already discussed, the delocalization of the π electrons over the cyclic architectures differ for the homoatomic and heteroatomic systems. Unlike carbon, nitrogen and phosphorus do not have a straightforward σ - π separation of their

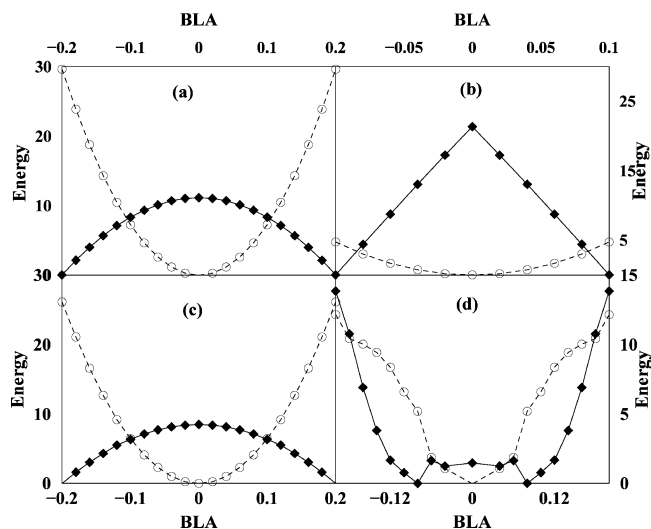


Figure 5. σ – π separation of energies for (a) C_6H_6 , (b) C_4H_4 , (c) $\text{B}_3\text{N}_3\text{H}_6$, and (d) $\text{N}_3\text{P}_3\text{F}_6$. Energies are reported in kcal/mol and BLA in Å. Circles and squares correspond to σ and π energies, respectively.

lower energy levels. Currently, there are efforts to understand aromaticity on the basis of the all-electron models where both σ and π electrons are explicitly taken into account and the overall structure is controlled by the predominance of either of the energy scales.²⁸ One of the most direct methods for considering the role of σ and π electrons is to separate the total energy of the system into σ and π components. For realizing the σ contribution to the structure, we consider the highest spin (H. S.) state for the systems and freeze all the π electrons in H. S. configuration. Thus, for the six-membered rings such as C_6H_6 , $\text{B}_3\text{N}_3\text{H}_6$, and $\text{N}_3\text{P}_3\text{F}_6$, the H. S. state corresponds to $S = 3$, while for the four-membered systems such as C_4H_4 , $\text{B}_2\text{N}_2\text{H}_4$, and $\text{N}_2\text{P}_2\text{F}_4$, the H. S. state has a spin of $S = 2$. The π energy for a system is calculated as $E(\pi) = E(\text{G. S.}) - E(\text{H. S.})$, where $E(\text{G. S.})$ corresponds to the energy of the singlet ($S = 0$) state. We have recently benchmarked this method of σ – π separation for both organic and inorganic molecules.²⁹

In Figure 5, we report this σ – π analysis for C_6H_6 , C_4H_4 , $\text{B}_3\text{N}_3\text{H}_6$, and $\text{N}_3\text{P}_3\text{F}_6$, as a function of distortion (BLA) in the rings using $\Delta E(\pi) = \Delta E(\text{G. S.}) - \Delta E(\text{H. S.})$, where the energies are scaled so that the most stable structure corresponds to the zero of energy. Note that we define $\Delta E(\text{H. S.}) = \Delta E(\sigma)$. For benzene (Figure 5a), the symmetric D_{6h} structure (0 BLA) is associated with the stabilization of the σ energy, while the π energy stabilizes the distorted structure. The energy scale for σ equalization overwhelms the π distortion (by 20 kcal/mol), and thus, the symmetric structure for benzene is stabilized. One can clearly observe the role of the σ energies in controlling the structure of benzene. Similar results have also been reported previously.³⁰ Contrary to the situation for benzene, C_4H_4 (Figure 5b) shows π distortion overwhelming σ equalization. Thus, the distorted D_{2h} structure is stabilized over the undistorted structure. Note that, for these homoatomic systems, we derive results identical to those well-known from π -only electron theories claiming benzene to be aromatic (0 BLA) and C_4H_4 to be JT-distorted antiaromatic.

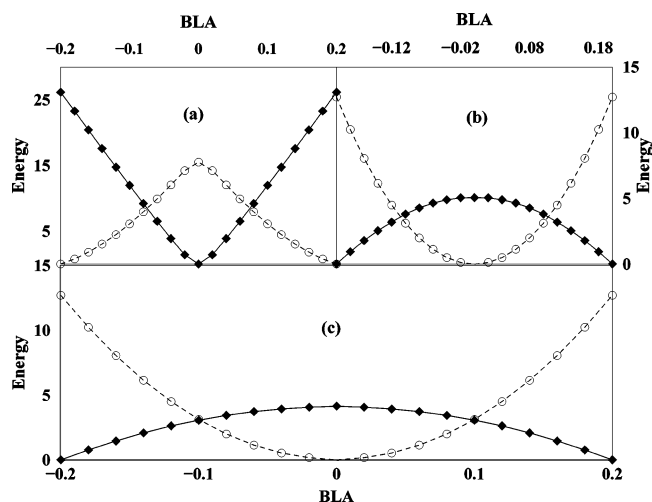


Figure 6. σ – π separation of energies for (a) $\text{N}_2\text{P}_2\text{F}_4$, (b) $\text{B}_2\text{N}_2\text{H}_4$ (planar), and (c) $\text{B}_2\text{N}_2\text{H}_4$ (puckered). Energies are reported in kcal/mol and BLA in Å. Circles and squares correspond to σ and π energies, respectively.

The heteroatomic B–N and P–N systems also show similar electronic features (Figure 5c and d). $\text{B}_3\text{N}_3\text{H}_6$ is identical to benzene in being σ -equalized and π -distorted. However, compared to benzene, the σ -equalization energy is smaller (by 5 kcal/mol), suggesting $\text{B}_3\text{N}_3\text{H}_6$ to be less aromatic, a result already derived from both NICS and topological analysis. $\text{N}_3\text{P}_3\text{F}_6$, on the contrary, shows double equalization, and both π and σ energies stabilize the 0 BLA structure. While, σ equalization is expected for a cyclic structure, π equalization suggests the predominating $p(\pi)$ – $d(\pi)$ delocalizations.

$\text{N}_2\text{P}_2\text{F}_4$ (Figure 6a), on the other hand, is σ -distorted but π -equalized (with π equalization $>$ σ distortion by 10 kcal/mol), suggesting strong π delocalization overwhelming minor JT distortion. Thus, $\text{N}_2\text{P}_2\text{F}_4$ may be considered as π -aromatic. In $\text{B}_2\text{N}_2\text{H}_4$, for both the planar (Figure 6b) and the puckered structures (Figure 6c), σ equalization overwhelms π distortion (by 10 kcal/mol). Thus, both the structures correspond to predominantly σ -aromatic 0 BLA geometries.

From the above σ – π analysis, it is clear that JT distortion in the backbones leads to structures with large BLAs. We have performed an analysis of the fragmentation of the total energy into contributions from the nuclear–nuclear (V_{nn}), electron–nuclear (V_{en}), electron–electron (V_{ee}), and kinetic energy (K.E) components as a function of BLA. The results for each of the systems are shown in Figure 7. For all cases, the electron–nuclear (V_{en}) component favors distortion, while V_{nn} , V_{ee} , and K.E have a preference for the undistorted structure. The V_{nn} , V_{ee} , and K.E components are stabilized in structures with 0 BLA as they are associated with a complete delocalization of electrons across the ring. For large BLAs, electrons are localized in the shorter bonds. Thus, the actual preference for the highly symmetric or distorted structure is governed by the competition between all other components and V_{en} . In C_6H_6 , V_{en} is overwhelmed by the other components (Figure 7a), while in the case of C_4H_4 , V_{en} is the major component (Figure 7b) and the structure is overall distorted. The preference for the heteroatomic systems such as $\text{B}_3\text{N}_3\text{H}_6$ (Figure 7c), $\text{B}_2\text{N}_2\text{H}_4$ (planar) (Figure 7d),

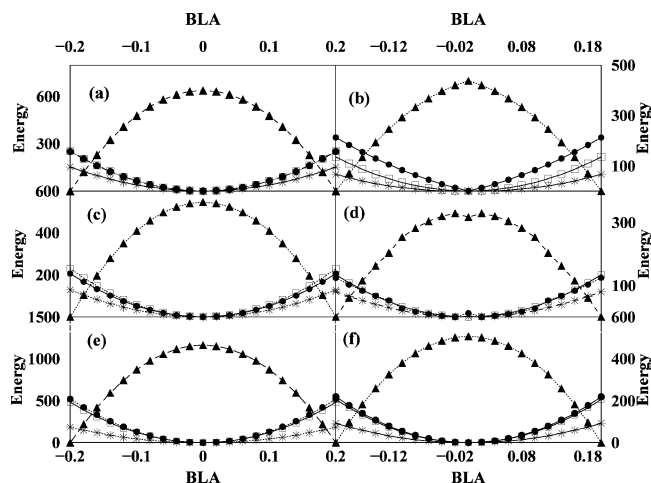


Figure 7. Variation of individual energy components (in kcal/mol) V_{ee} (circles), V_{nn} (squares), V_{ne} (triangles), and V_{KE} (stars) with BLA in Å for (a) C_6H_6 , (b) C_4H_4 , (c) $B_3N_3H_6$, (d) $B_2N_2H_4$ (planar), (e) $N_3P_3F_6$, and (f) $N_2P_2F_4$.

$N_3P_3F_6$ (Figure 7e), and $N_2P_2F_4$ (Figure 7f) adapting to a highly symmetric structure (0 BLA) is also clearly understood from the fact that, for these systems, V_{en} is only a minor component.

V. Conclusions

We have considered aromaticity and antiaromaticity in various molecules. Organic molecules such as C_6H_6 and C_4H_4 are stabilized through isotropic delocalization of the π electrons over the full perimeter of the rings. The CT and $p(\pi)-d(\pi)$ interactions in $B_3N_3H_6$ and $N_3P_3F_6$, respectively, lead to aromaticity in these systems although the aromatic character is less than that of benzene. Four-membered heteroatomic systems such as $N_2P_2F_4$ and $B_2N_2H_4$ are also aromatic.

Apart from the covalently bonded systems, the weakly interacting H-bonded systems also have aromatic characteristics. In fact, it is the weak aromaticity developed as a result of the nonlocal nature of these interactions that stabilizes such systems. Finally, we propose that aromaticity is a single parameter that includes all specific interactions in the weakly interacting cyclic systems and provides a global tool to understand their structures.

Acknowledgment. S.S.M. thanks CSIR for the research fellowship. S.K.P. acknowledges CSIR and DST, Government of India, for the research grants.

Supporting Information Available: Cartesian coordinates, total energy (in Hartrees), frequency calculations for all the structures, and complete reference 19. This material is available free of charge via the Internet at <http://pubs.acs.org>.

References

- (1) (a) Minkin, V. I.; Glukhovtsev, M. N.; Simkin, B. Y. *Aromaticity and Antiaromaticity*; Wiley: New York, 1994. (b) Shaik, S.; Shurki, A.; Danovich, D.; Hilbert, P. C. *Chem. Rev.* **2001**, *101*, 1501–1539. (c) Gomes, J. A. N. F.; Mallion, R. B. *Chem. Rev.* **2001**, *101*, 1349–1383.

- (2) (a) Mesbah, W.; Prasang, C.; Hofmann, M.; Geiseler, G.; Massa, W.; Berndt, A. *Angew. Chem., Int. Ed.* **2003**, *42*, 1717–1719. (b) Schiemenz, B.; Huttner, G. *Angew. Chem., Int. Ed. Engl.* **1993**, *32*, 297.
- (3) (a) Takanashi, K.; Lee, V. Y.; Matsuno, T.; Ichinohe, M.; Sekiguchi, A. *J. Am. Chem. Soc.* **2005**, *127*, 5768–5769. (b) Lee, V. Y.; Matsuno, T.; Ichinohe, M.; Sekiguchi, A. *J. Am. Chem. Soc.* **2004**, *126*, 4758–4759.
- (4) (a) Li, X.; Kuznetsov, A.; Zhang, H.-F.; Boldyrev, A. I.; Wang, L. *Science* **2001**, *291*, 859–861. (b) Li, X.; Zhang, H.-F.; Wang, L.-S.; Kuznetsov, A. E.; Cannon, N. A.; Boldyrev, A. I. *Angew. Chem., Int. Ed.* **2001**, *40*, 1867–1870. (c) Kuznetsov, A.; Boldyrev, A. I.; Li, X.; Wang, L.-S. *J. Am. Chem. Soc.* **2001**, *123*, 8825–8831.
- (5) (a) Kuznetsov, A. E.; Birch, K.; Boldyrev, A. I.; Li, X.; Zhai, H.; Wang, L. *Science* **2003**, *300*, 622–625. (b) Chen, Z.; Corminboeuf, C.; Heine, T.; Bohmann, J.; Schleyer, P. v. R. *J. Am. Chem. Soc.* **2003**, *125*, 13930–13931.
- (6) (a) Wannere, C. S.; Corminboeuf, C.; Wang, Z.-X.; Wodrich, M. D.; King, R. B.; Schleyer, P. v. R. **2005**, *127*, 5701–5705. (b) Santos, J. C.; Tiznado, W.; Contreras, R.; Fuentealba, P. *J. Chem. Phys.* **2004**, *120*, 1670. (c) Santos, J. C.; Andres, J.; Aizman, A.; Fuentealba, P. *J. Chem. Theory Comput.* **2005**, *1*, 83.
- (7) (a) Heilbronner, E. *Tetrahedron Lett.* **1964**, *29*, 1923–1928. (b) Ajami, D.; Oeckler, O.; Simon, A.; Herges, R. *Nature* **2003**, *426*, 819–821. (c) Kawase, T.; Oda, M. *Angew. Chem., Int. Ed.* **2004**, *43*, 4396–4398.
- (8) (a) Jutzi, P.; Mix, A.; Rummel, B.; Schoeller, W. W.; Neumann, B.; Stamm, H.-G. *Science* **2004**, *305*, 849. (b) Datta, A.; Pati, S. K. *J. Am. Chem. Soc.* **2005**, *127*, 3496–3500.
- (9) (a) Rio, D. D.; Galindo, A.; Resa, I.; Carmona, E. *Angew. Chem., Int. Ed.* **2005**, *44*, 1244–1247. (b) Resa, I.; Carmona, E.; Gutierrez-Puebla, E.; Monge, A. *Science*, **2004**, *305*, 1136. (c) Xie, Y.; Schaefer, H. F., III; King, R. B. *J. Am. Chem. Soc.* **2005**, *127*, 2818–2819.
- (10) March, J. *Advanced Organic Chemistry: Reactions, Mechanisms and Structure*, 4th edition; John Wiley and Sons: New York, 1992.
- (11) (a) Allcock, H. R. *Chem. Rev.* **1972**, *72*, 315. (b) Kiran, B.; Phukan, A. K.; Jemmis, E. D. *Inorg. Chem.* **2001**, *40*, 3615–3618. (c) Boyd, R. J.; Choi, S. C.; Hale, C. C. *Chem. Phys. Lett.* **1984**, *112*, 136. (d) Jemmis, E. D.; Kiran, B. *Inorg. Chem.* **1998**, *37*, 2110–2116. (e) Krishnamurthy, S. S.; Sau, A. C.; Woods, M. *Adv. Inorg. Chem. Radiochem.* **1978**, *21*, 41–112. (f) Soncini, A.; Domene, C.; Engelberts, C. C.; Fowler, P. W.; Rassat, A.; Lenthe, J. H.; Havenith, R. W. A.; Jenneskens, L. W. *Chem. Eur. J.* **2005**, *11*, 1257–1266.
- (12) (a) Baceiredo, A.; Bertrand, G.; Majoral, J.-P.; Sicard, G.; Juad, J.; Galy, J. *J. Am. Chem. Soc.* **1984**, *106*, 6088–6089.
- (13) (a) Stone, A. J. *The Theory of Intermolecular Forces*; Oxford University Press: New York, 1996. (b) Ratajczak, H.; Orville-Thomas, W. J. *Molecular Interactions*; John Wiley and Sons: New York, 1980.
- (14) (a) Steiner, T. *Angew. Chem., Int. Ed. Engl.* **2002**, *41*, 48. (b) Desiraju, G. R.; Steiner, T. *The Weak Hydrogen Bond in Structural Chemistry and Biology*; Oxford University Press: New York, 1999.
- (15) (a) Etter, M. C. *Acc. Chem. Res.* **1990**, *23*, 120. (b) Etter, M. C.; MacDonald, J. C.; Bernstein, J. *Acta Crystallogr., Sect. B* **1990**, *46*, 256.

- (16) (a) Radhakrishnan, T. P.; Herndon, W. C. *J. Phys. Chem.* **1991**, 95, 10609. (b) Bernstein, J.; Davis, R. E.; Shimoni, L.; Chang, N.-L. *Angew. Chem., Int. Ed. Engl.* **1995**, 34, 1555.
- (17) Scheiner, S. *Hydrogen Bonding: A Theoretical Perspective*; Oxford University Press: New York, 1997.
- (18) (a) Becke, A. D. *J. Chem. Phys.* **1993**, 98, 1372. (b) Lee, C.; Yang, W.; Parr, R. G. *Phys. Rev. B* **1988**, 37, 785.
- (19) *Gaussian 03*, revision B.05; Gaussian, Inc.: Pittsburgh, PA, 2003.
- (20) *Conquest*, version 1.7; Cambridge Crystallographic Database, Cambridge Crystallographic Data Centre: Cambridge, U. K., 2004.
- (21) Paetzold, P.; Richter, A.; Thijssen, T.; Wurtenberg, S. *Chem. Ber.* **1979**, 112, 3811.
- (22) Paetzold, P.; von Plotho, C.; Schmid, G.; Boese, R.; Schrader, B.; Bougeard, D.; Pfeiffer, U.; Gleiter, R.; Schafer, W. *Chem. Ber.* **1984**, 117, 1089.
- (23) Schleyer, P. v. R.; Maerker, C.; Dransfeld, A.; Jiao, H.; Eikema-Hommas, N. J. R. v. *J. Am. Chem. Soc.* **1996**, 118, 6317.
- (24) (a) Bader, R. F. W. *Atoms in Molecules: A Quantum Theory*; Clarendon Press: Oxford, U. K., 1995. (b) Cole, J. M.; Copley, R. C. B.; McInyre, G. J.; Howard, J. A. K.; Szablewski, M.; Cross, G. H. *Phys. Rev. B* **2002**, 65, 125107–(1–11). (c) Ranganathan, A.; Kulkarni, G. U. *Proc. Indian Acad. Sci., Chem. Sci.* **2003**, 115, 637–647. (d) Luana, V.; Pendas, A. M.; Costales, A.; Carriedo, G. A.; G-Alonson, F. J. *J. Phys. Chem. A* **2001**, 105, 5280–5291.
- (25) (a) Hobza, P.; Zahradnik, R. *Chem. Rev.* **1988**, 88, 871. (b) Boys, S. F.; Bernardi, F. *Mol. Phys.* **1970**, 19, 553.
- (26) (a) Gilli, G.; Bellucci, F.; Ferretti, V.; Bertolasi, V. *J. Am. Chem. Soc.* **1989**, 111, 1023. (b) Mohajeri, A. *THEOCHEM*, **2004**, 678, 201. (c) Bertolasi, V.; Gilli, P.; Ferretti, V.; Gilli, G. *J. Am. Chem. Soc.* **1991**, 113, 4917. (d) Wojtulewski, S.; Grabowski, S. J. *THEOCHEM*, **2003**, 621, 285.
- (27) (a) Dannenberg, J. J.; Rios, R. *J. Phys. Chem.* **1994**, 98, 6714. (b) Craw, J. S.; Bacskey, G. B. *J. Chem. Soc., Faraday Trans.* **1992**, 88, 2315. (c) Gilli, P.; Bertolasi, V.; Ferretti, V.; Gilli, G. *J. Am. Chem. Soc.* **1994**, 116, 909.
- (28) (a) Jug, K.; Hilbert, P. C.; Shaik, S. *Chem. Rev.* **2001**, 101, 1477. (b) Jug, K.; Koster, A. M. *J. Am. Chem. Soc.* **1990**, 112, 6772.
- (29) Datta, A.; Pati, S. K. *J. Chem. Theory Comput.* **2005**, 1, 824.
- (30) Shaik, S.; Hilbert, P. C. *J. Am. Chem. Soc.* **1985**, 107, 3089.

CT0501598